ACS OMEGA

http://pubs.acs.org/journal/acsodf

Article

Enhanced Antimicrobial Activity of Biofunctionalized Zirconia Nanoparticles

Mujeeb Khan,* Mohammed Rafi Shaik, Shams Tabrez Khan, Syed Farooq Adil, Mufsir Kuniyil, Majad Khan, Abdulrahman A. Al-Warthan, Mohammed Rafiq H. Siddiqui, and Muhammad Nawaz Tahir*

Cite This: *ACS Omega* 2020, 5, 1987−1996

Read Online

ACCESS | Metrics & More | Article Recommendations | Supporting Information

ABSTRACT: The effective interactions of nanomaterials with biological constituents play a significant role in enhancing their biomedicinal properties. These interactions can be efficiently enhanced by altering the surface properties of nanomaterials. In this study, we demonstrate the method of altering the surface properties of ZrO_2 nanoparticles (NPs) to enhance their antimicrobial properties. To do this, the surfaces of the ZrO_2 NPs prepared using a solvothermal method is functionalized with glutamic acid, which is an α-amino acid containing both COO^- and NH_4^+ ions. The binding of glutamic acid (GA) on the surface of ZrO_2 was confirmed by UV−visible and Fourier transform infrared spectroscopies, whereas the phase and morphology of resulting GA-functionalized ZrO_2 (GA-ZrO_2) was identified by X-ray diffraction and transmission electron microscopy. GA stabilization has altered the surface charges of the ZrO_2, which enhanced the dispersion qualities of NPs in aqueous media. The as-prepared GA-ZrO_2 NPs were evaluated for their antibacterial properties toward four strains of oral bacteria, namely, *Rothia mucilaginosa*, *Rothia dentocariosa*, *Streptococcus mitis*, and *Streptococcus mutans*. GA-ZrO_2 exhibited increased antimicrobial activities compared with pristine ZrO_2. This improved activity can be attributed to the alteration of surface charges of ZrO_2 with GA. Consequently, the dispersion properties of GA-ZrO_2 in the aqueous solution have increased considerably, which may have enhanced the interactions between the nanomaterial and bacteria.

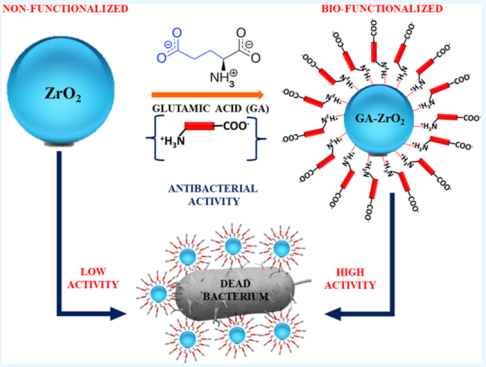

1. INTRODUCTION

Recently, the emergence of bacterial resistance to conventional antibacterial drugs has become the greatest health challenge in the medical field.[1,2] One of the serious concerns of such bacterial resistance is the potential recurrence of infectious diseases that were effectively controlled for several decades.[3,4] In many cases, the drug resistance has led to the prescription of high doses of antibiotics, which often generate unbearable toxicity.[5] In this scenario, the development of unconventional strategies to treat infectious diseases has become highly desirable.[6] Among several alternatives, the applications of nanoscale materials, such as metal and metal oxide nanoparticles (NPs), as antimicrobial agents have attracted considerable attention.[7,8] Owing to their excellent physicochemical properties, including a high surface-to-volume ratio, NPs have exhibited superb antibacterial properties.[9] Particularly, metal oxide NPs, which are biocompatible and noncytotoxic, have great prospects as antimicrobial agents.[10,11]

The antimicrobial properties of nanomaterials are based on several factors including size, stability, and their concentration in the growth medium.[12−14] Furthermore, morphology, surface charge, and surface coating of NPs also play a critical role in determining the antimicrobial properties of nanomaterials.[15−18]

In addition, the stability and dispersibility/solubility of the NPs in the nutrient medium also has significant influence on the bacterial growth. Increased dispersibility provides sufficient time for the proper interaction between bacteria and NPs.[19,20] NPs are generally stabilized by their surface functionalization using different types of stabilizing agents, which bind to the surface of NPs through specific interactions.[21] The surface functionalization of NPs effectively inhibits their aggregation due to the enhanced stability and high water solubility.[22−24] Therefore, the antimicrobial activity of the NPs can be considerably improved by the appropriate selection of functionalizing agents.[25] So far, the effect of functionalizing agents on the antimicrobial activities of the NPs, such as the nature of the stabilizing ligands, their concentration, and many other factors, has been rarely studied. In our previous study, we

Received: November 12, 2019
Accepted: January 13, 2020
Published: January 23, 2020

https://dx.doi.org/10.1021/acsomega.9b03840
ACS Omega 2020, 5, 1987−1996

Scheme 1. Schematic Representation of the Biofunctionalization of ZrO_2 NPs with Glutamic Acid and Their Enhanced Antibacterial Properties

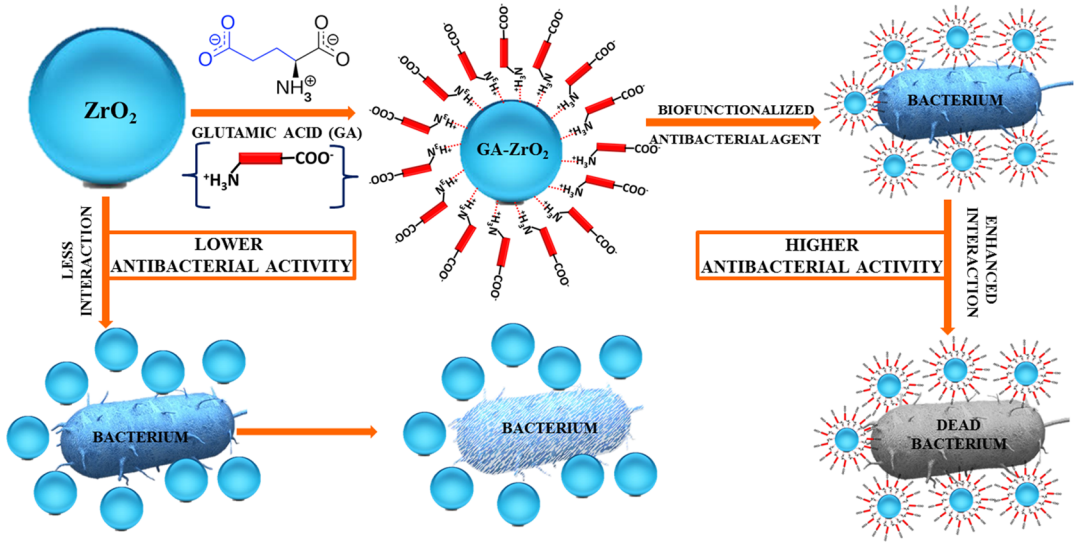

have demonstrated the effect of the concentration of stabilizing ligands on the antimicrobial activity of silver NPs.[26]

In this regard, a number of different stabilizing agents such as alcohols, polyols, polyether, carbohydrates, water-soluble polymers, and polysaccharides have been used to enhance the functional activity of NPs.[27] However, the toxic nature of several chemical ligands has seriously affected their biocompatibility; therefore, proper choice of biologically active biomolecules for stabilizing the surface of these NPs will surely enhance their biocompatibility and biological applicability.[28] Besides, it also helps to curtail the nonspecific toxicity of NPs.[29] Therefore, rational selection of therapeutically active biomolecules for the functionalization of NPs will surely enhance their biological applicability.[30] The conjugation of biomolecules with NPs not only provides stabilization of the system but also introduces biocompatible functionalities onto these NPs for further biological interactions or coupling.[31] One such biomolecule is the L-glutamic acid, which is a natural α-amino acid and is readily available.[32] Due to its biocompatible nature, it has various biomedical and pharmacological applications. Particularly, due to its extraordinary binding ability, glutamic acid is extensively used as a renewable surfactant in various industrial applications.[33] Furthermore, various glutamic acid-based biopolymers have been used as ligands for the surface modifications of NPs to enhance their biological properties.[34,35] So far, the surface modifications of various metallic NPs with an aim to provide stable biomolecule-functionalized nanomaterials for antimicrobial applications have been reported.[36−38] However, in comparison to the reports on the antimicrobial activities of metallic NPs, very limited information is available on the antimicrobial properties of metal oxide NPs.[39]

Several metal oxides such as ZnO, TiO_2, Fe_2O_3, CuO, etc. are known to possess superior antimicrobial properties.[40−42] However, limited studies have been reported on the bactericidal properties of zirconium dioxide (ZrO_2). Various ZrO_2-based materials exhibit excellent biological responses due to their superior mechanical properties and excellent biocompatibility. Indeed, in some cases, these materials are also effective at reducing the viability of adherent bacteria such as *Streptococcus sanguinis* and *Porphyromonas gingivalis* and thus have been widely used in dental materials, implants, etc.[43] Albeit, some of zirconium-based mixed ligand complexes have been shown to possess considerable antimicrobial properties.[44,45] However, pristine ZrO_2 exhibit negligible biocidal properties, which have been often enhanced by combining with other biologically active materials.[46,47] In this regard, surface modification of ZrO_2 has often been carried out using various physical and chemical methods to enhance the bioactivity of the resultant material.[48] Therefore, development of simple and effective methods for the surface modification of ZrO_2 to enhance its bioactivity is highly desirable.

In this study, we have demonstrated the synthesis of cubic ZrO_2 NPs and a method of their biofunctionalization using L-glutamic acid as ligands. The as-obtained biofunctionalized NPs were characterized using various techniques, such as X-ray diffraction (XRD), ultraviolet−visible (UV−vis), and Fourier transform infrared (FT-IR) spectroscopies and high-resolution transmission electron microscopy (HR-TEM). Furthermore, we have also investigated the effect of glutamic acid on the antibacterial properties of ZrO_2 NPs. For this purpose, the antibacterial properties of both pristine ZrO_2 NPs and their biofunctionalized counterparts were tested against various bacterial strains such as, *Rhodotorula muciliginosa* (*R. muciliginosa*), *Rothia dentocariosa* (*R. dentoicariosa*), *Streptococcus mitis* (*S. mitis*), and *Streptococcus mutans* (*S. mutans*) bacteria (cf. Scheme 1).

2. RESULTS AND DISCUSSION

2.1. UV−Vis Analysis. For this study, ZrO_2 NPs were obtained by applying solvothermal conditions using benzyl alcohol as the solvent.[49,50] In this case, benzyl alcohol not only facilitated the formation of ZrO_2 NPs but it also stabilized the surfaces of the NPs. However, when the antimicrobial activity of the benzyl alcohol-stabilized ZrO_2 NPs was tested, the NPs have demonstrated very low antimicrobial activity. In order to increase the antimicrobial potency of pristine ZrO_2 NPs, the as-prepared ZrO_2 NPs were functionalized with a biomolecule named glutamic acid (GA). GA is an α-amino acid, which is used in the biosynthesis of proteins in living organisms. It possesses both cationic ($-NH^+$) and anionic groups

https://dx.doi.org/10.1021/acsomega.9b03840
ACS Omega 2020, 5, 1987−1996

(−COO$^-$), which significantly enhances its electrostatic and ionic/hydrogen bonding interactions with other biomaterials.[51] Therefore, GA was selected as the stabilizing ligand to enhance the dispersibility to prevent agglomeration of ZrO_2 NPs in the aqueous medium and also to increase the biocompatibility of the resulting material.[52] Initially, the functionalization of ZrO_2 NPs was confirmed with UV measurements. For this purpose, the UV spectra of glutamic acid (GA, red line), pristine ZrO_2 (blue line), and GA-ZrO_2 (green line) were recorded as shown in Figure 1. Typically, GA (red line) and ZrO_2 do not have any

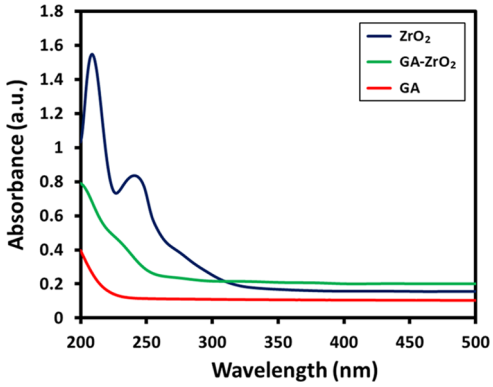

Figure 1. UV−vis absorption spectra of ZrO_2 NPs (blue line), GA-ZrO_2 (green line), and GA (red line).

characteristic UV peaks, whereas benzyl alcohol exhibits two prominent peaks at 215 and 262 nm.[49] Therefore, the UV spectrum of benzyl alcohol-stabilized ZrO_2 in Figure 1 (blue line) also shows these peaks. However, these two peaks disappear significantly upon functionalization with GA, which clearly indicates the successful exchange of benzyl alcohol with GA as a stabilizing ligand on the surface of ZrO_2 (green line).

2.2. FT-IR, TGA, and XRD Analysis. The presence of GA on the surface of ZrO_2 is also confirmed by FT-IR analysis (cf. Figure 2). The IR spectrum of ZrO_2 (Figure 2, blue line) shows various intense peaks in the range of 500−850, etc., which are attributed to the Zr−O bond. Additionally, the spectrum also contains several other IR peaks, which can be associated to the presence of benzyl alcohol on the surface of ZrO_2 NPs.[49] For instance, the absorption bands between 1785 and 1620 cm^{-1} correspond to the combination bands of the

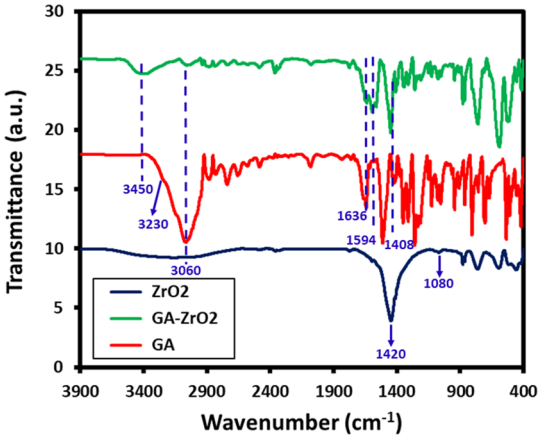

Figure 2. FT-IR spectra of ZrO_2 NPs (blue line), GA- ZrO_2 (green line), and GA (red line).

phenyl rings. The bands between 1420−1330 cm^{-1} and 1080−1022 cm^{-1} are characteristic for the O−H and C−O stretches of benzyl alcohol. Whereas, the IR spectrum of glutamic acid (Figure 2, red line) consists of various absorption bands, such as at ∼3000−3250 cm^{-1} (N−H stretching, characteristic of amino acids), 1550−1650 (N−H bending vibrations and amino acid zwitterions), ∼2890 cm^{-1} (C−H stretching), ∼2081 (N−H stretching), ∼1640 cm^{-1} (carboxylate vibration), 1710−1730 cm^{-1} (C═O stretching), 1250−1050 (C−N stretching), etc.[53] On the other hand, the spectrum of GA-ZrO_2 (Figure 2, green line) consists of various IR peaks, which belong to both GA and ZrO_2; this clearly indicates that GA has successfully replaced the benzyl alcohol as a stabilizing ligand on the surface of ZrO_2. Generally, the chelating ligands (such as glutamic acid) bind the surface of metal oxide nanoparticles through their chelation with undercoordinated metal ions present on the surface of nanoparticles.[54,55] As shown in Scheme 1, the glutamic acid chelates the ZrO_2 nanoparticles through the α-amino carboxylic acid side. The FT-IR spectra of pure glutamic acid (Figure 2, redline) show the spectra, which represent the zwitterionic nature of the α-amino carboxylic acid side with $-NH_3^+$ stretching absorption between 3230 and 3060 cm^{-1}.[56] After chelation on the surface of ZrO_2 nanoparticles, this band almost disappears, and a new broad band centered at 3450 cm^{-1} appears, which could be due to side chain COOH or the remaining chelated NH groups. In comparison with the FTIR spectrum of pure glutamic acid, there are noticeable shifts in the region from 1700−1250 cm^{-1}. These also suggest that the α-amino-carboxylic acid side binds the ZrO_2 nanoparticle surface. After functionalization, the crystallinity of GA-ZrO_2 remained unaffected as confirmed by the XRD spectrum shown in Figure 3. Glutamic acid is known to crystallize in two forms,

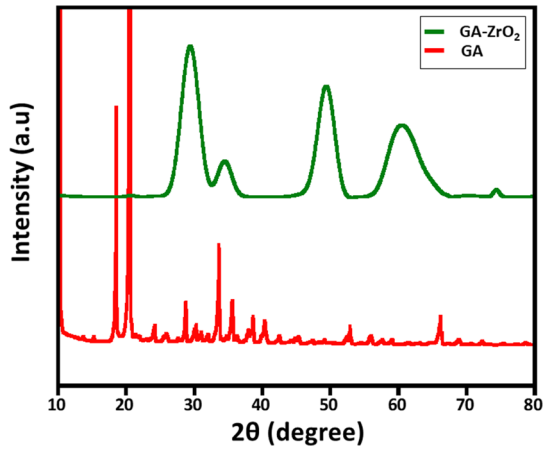

Figure 3. XRD diffractogram pattern of GA and GA-ZrO_2.

the metastable α-form and the stable β-form. Both forms crystallize in the orthorhombic unit cell ($P2_12_12_1$).[57] The XRD spectrum of pure GA in Figure 3, (red line) indicates toward the stable β-form of the GA due to presence of characteristic diffraction peaks between 10 to 25°.[58] Whereas, the XRD pattern of GA-ZrO_2 (Figure 3, green line) remained unaffected and rendered the same diffraction peaks as that of pure ZrO_2 (data is provided in the Supporting Information, Figure S5), which correspond to the cubic phase of ZrO_2. The pattern contains five characteristic peaks at 2θ values of 30.46, 34.54, 50.45, 60.37, and 74.56° belonging to the (111), (200), (220),

https://dx.doi.org/10.1021/acsomega.9b03840
ACS Omega 2020, 5, 1987−1996

(311), and (400) planes of crystalline zirconia. Notably, glutamic acid might have bound to the surfaces of ZrO_2 nanoparticles in the form of a monolayer, which is similar to self-assembled monolayers (SAMs) on 2D substrates. Although, in bulk, glutamic acid can self-assemble in the solid state and diffract under X-ray beam with an identical diffractogram, but on the surfaces of nanoparticles in the form of a monolayer, it does not show any reflection.[59] The glutamic acid-stabilized silver nanoparticles also showed no extra reflections as reported by Chandra and Singh.[60] Furthermore, the biofunctionalization of ZrO_2 NPs is also confirmed by TGA analysis. The TGA traces of pure glutamic acid, pristine ZrO_2, and GA-ZrO_2 are shown in Figure 4. In pure glutamic

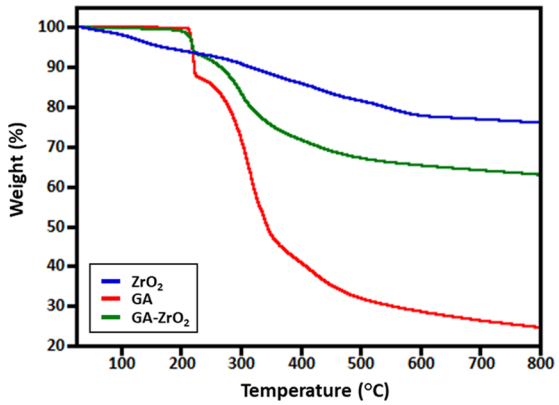

Figure 4. TGA analysis of GA, ZrO_2, and GA-ZrO_2.

acid, the first sudden weight loss of ~15% up to 200 °C is accounted for the removal of moisture and trapped water. This is followed by another gradual weight loss of_~55% from 200 to 300 °C, which was assigned to the thermal elimination of labile carbon and oxygen moieties of glutamic acid. On the other hand, pristine ZrO_2 exhibited a gradual weight loss of only ~20% up to 800 °C in a single step. Whereas, GA-ZrO_2 has demonstrated a weight loss of ~30% in a similar fashion in two different steps as observed in pure glutamic acid. This indicates the presence of organic moieties on the surface of ZrO_2 after the functionalization with glutamic acid.

2.3. Dispersibility and Surface Charge Properties. One of the key challenges for the biological applications of metal or metal oxide-based nanomaterials is maintaining the stability of the nanoparticles in aqueous media. Since nanomaterials used in biological applications including toxicology studies are usually received in powder form, therefore, preparation of high-quality dispersion of these materials is often required for in vitro and in vivo tests. Furthermore, stable dispersion of nanoparticles provides a versatile and well-defined interface, which allows sufficient contact with biomaterials. To ascertain the stability of both pristine ZrO_2 and GA-ZrO_2 in the aqueous media, the zeta potential of the four different samples ZrO_2 were measured, including pristine ZrO_2, ZrO_2 at pH 8, and GA-ZrO_2 and GA-ZrO_2 at pH 8, as the biological properties of NPs were measured at this pH. Moreover, pH has strong influence on the zeta potential values, and a slight change in pH can significantly alter the quality of dispersion. The zeta potentials of ZrO_2, ZrO_2 at pH 8, and GA-ZrO_2 and GA-ZrO_2 at pH 8 were found to be −1.78, −11.9, −1.33, and −33.9, respectively. The zeta potential plots of all these samples are provided in the Supporting Information Figures S1−S4. The zeta potential identifies the charges on the surface of NPs (negative or positive) and their magnitude, which typically varied depending upon the type of ligands used during the synthesis.[61] Typically, nanoparticles consisting of near-neutral zeta potential or mildly charged surfaces tend to aggregate faster, which implies that the stronger the charge, the better is the colloidal stability of the particles.[62] Glutamic acid consists of two carboxyl groups (−COOH) and one amino group (−NH), and when it is dissolved in water, the amino group ($-NH_2$) may gain a proton (H^+), and/or the carboxyl groups may lose protons, depending on the pH of the medium. Especially at higher pH, (>7) both the carboxylic acid groups lose their proton, and the acid exists almost entirely as the glutamate anion ($^-OOC-CH(NH^+_3)-(CH_2)_2-COO^-$) with a single negative charge overall.[63] Both pure ZrO_2 and GA-ZrO_2 NPs have displayed near-neutral zeta potentials, which point toward their lower aqueous stabilities. However, when the zeta potential of these samples was measured at pH 8, the values increased significantly, which clearly indicated toward the enhanced stability of the samples at this pH. Notably, the GA-stabilized ZrO_2 has demonstrated a much larger potential value when compared to the pure ZrO_2 at pH 8, which can be attributed to the better stabilizing properties of GA due to the presence of strong negative charge of glutamate ions. This was further confirmed by investigating the dispersibility of ZrO_2 and GA-ZrO_2 in the aqueous solution at both neutral and higher pH. For this purpose, freshly produced ZrO_2 and GA-ZrO_2 were dispersed in DI water by sonicating a 5 mg sample in 10 mL water. The samples of high pH values were also prepared in a similar fashion in which the pH was adjusted by using a diluted NaOH solution. Both the ZrO_2 and GA-ZrO_2 have demonstrated lower dispersibility at neutral pH; however, at a higher pH of 8, the samples have shown enhanced dispersibility as shown in Figure 5; this is consistent with

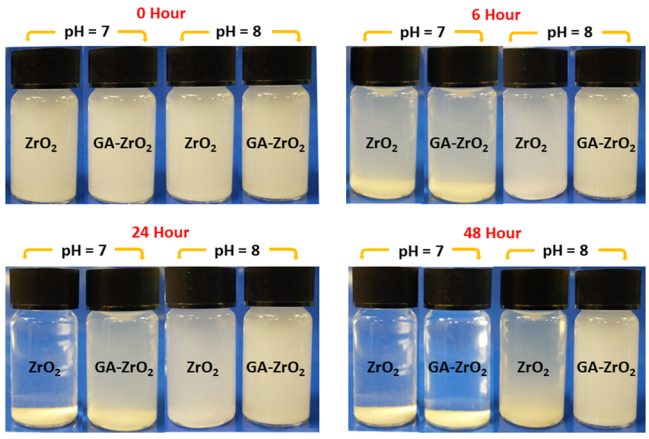

Figure 5. Digital images of the dispersions of ZrO_2 and GA-ZrO_2 at neutral pH (7) and higher pH (8).

results of zeta potential. Indeed, GA-ZrO_2 at pH 8, which possesses highest zeta potential (−33.9), has shown superior dispersion quality when compared to all other samples.

2.4. TEM Analysis. Size and dispersibility of GA-ZrO_2 NPs was further confirmed using transmission electron microscopy (TEM) as shown in Figure 6. The nanoparticles are very small with an average diameter around 2.5 nm (Figure 6D) and monocrystalline as shown by well-defined *d*-spacing. The

https://dx.doi.org/10.1021/acsomega.9b03840
ACS Omega 2020, 5, 1987−1996

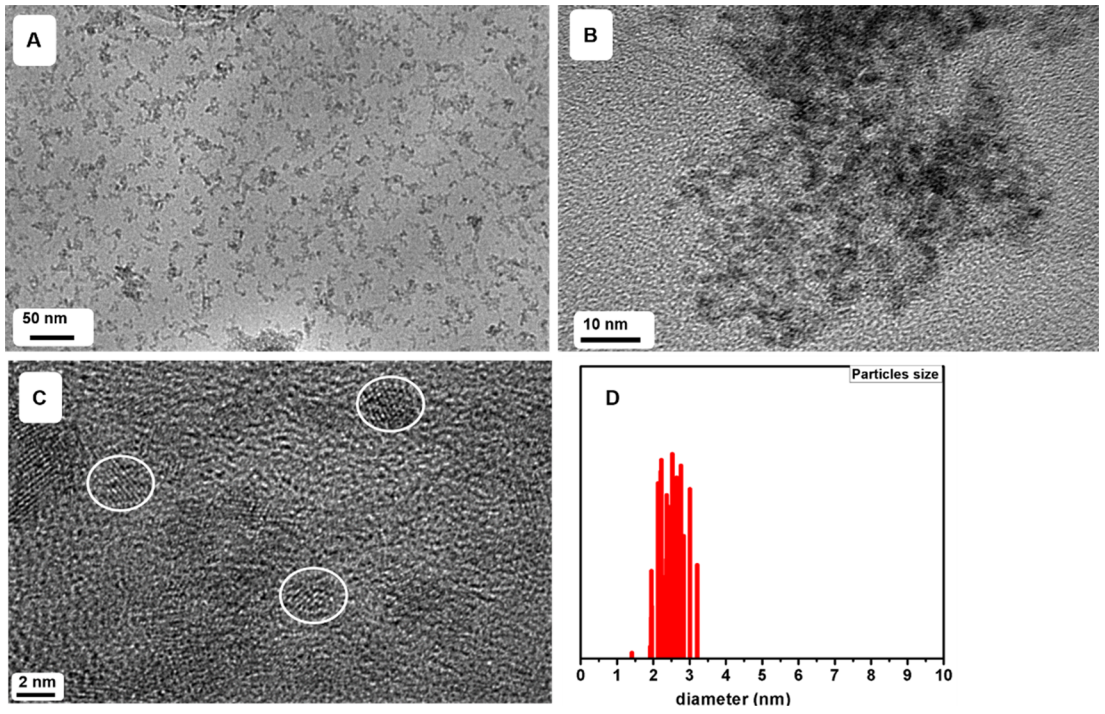

Figure 6. TEM micrograph indicating the size, crystallinity, and dispersibility of GA-ZrO_2 nanoparticles. (a−c) TEM images of GA-ZrO_2 at different resolutions and (d) particle size distribution of GA-ZrO_2. The TEM images of pure ZrO_2 NPs are provided in the Supporting Information Figure S6.

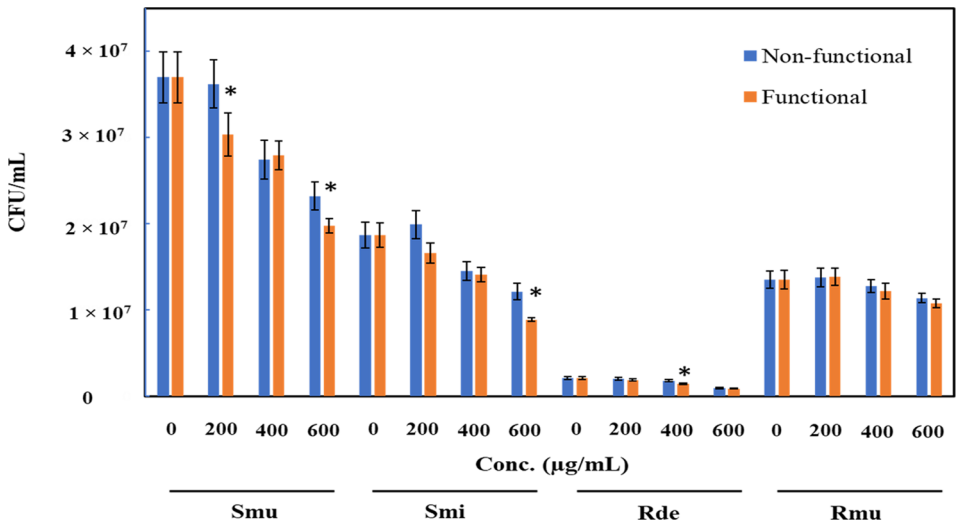

Figure 7. Decrease in the population of oral pathogens (Smu, *Streptococcus mutans*; Smi, *Streptococcus mitis*; Rde, *Rothia denticoriosa*; and Rmu, *Rothia muciliginosa*) when grown with various concentrations of functionalized ZrO_2 (orange bars) compared to non-functionalized ZrO_2.

nanoparticles are well-isolated (as indicated by white circles, Figure 6C) on the TEM grid, confirming the dispersibility of GA-ZrO_2 in aqueous mediums.

2.5. Antimicrobial and Anti-Biofilm Activities. In general, the growth of all the tested strains was inhibited due to the presence of both functionalized (GA-ZrO_2) and non-functionalized (ZrO_2) zirconia. Interestingly, GA-ZrO_2 has demonstrated an enhanced antimicrobial activity toward all the strains studied. The highest inhibition of the growth (58% ± 4.9%) was observed against *R. dentoicariosa* by GA-ZrO_2 at 600 ug/mL (Figure 7). It was observed that the antimicrobial activity increased by ∼11% due to the functionalization, which is a significant change. Similarly, the growth of *S. mutans* also decreased by 52% ± 2.9% and by 35.2% ± 7.9% with functionalized and non-functionalized zirconia, respectively. Here, it is also observed that due to the functionalization, the antimicrobial activity increased by 17%. However, *R. muciliginosa* was least sensitive to both functionalized and non-functionalized zirconia. For this strain, a very small change in the activity was observed due to the functionalization. It is however interesting to note that the antimicrobial activity of the functionalized zirconium increased against the oral pathogenic strains.

2.6. Antibiofilm Activity. When the anti-biofilm activities in the presence of functionalized and non-functionalized zirconia were checked, significant reduction of the biofilm

https://dx.doi.org/10.1021/acsomega.9b03840
ACS Omega 2020, 5, 1987−1996

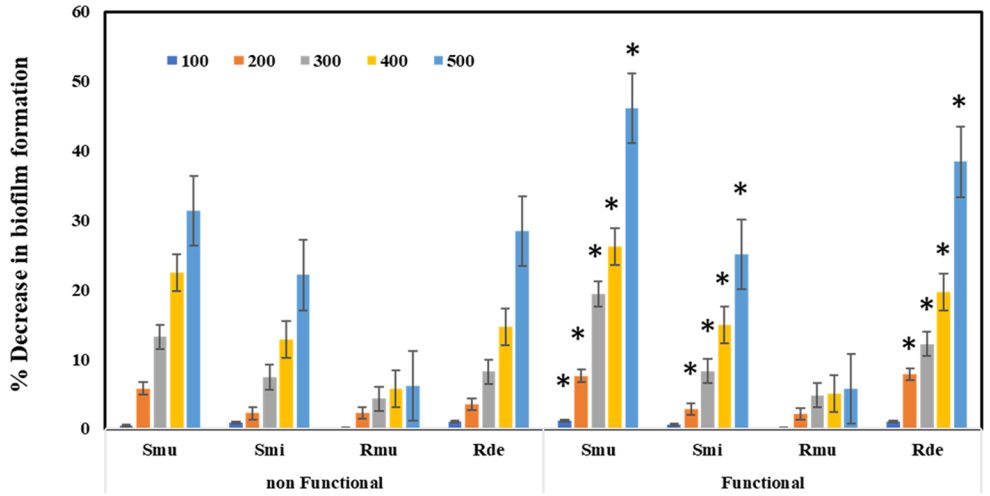

Figure 8. Decrease in the biofilm formation by oral pathogens (Smu, *Streptococcus mutans*; Smi, *Streptococcus mitis*; Rde, *Rothia denticoriosa*; and Rmu, *Rothia muciliginosa*) when grown with various concentrations (100, 200, 300, 400, and 500 μg/mL) of functionalized ZrO_2 (GA-ZrO_2) compared to non-functionalized ZrO_2.

was observed in *R. dentoicariosa* and *S. mutans*, wherein a decrease of 46 and 38%, respectively, was observed. However, the biofilm formation activity of *R. muciliginosa* was not affected. When the difference between the biofilm formation activity of functional and non-functional zirconium was compared, it was observed that the anti-biofilm activity of the functionalized zirconium increased slightly. It is to be noted that the maximum increase of 10% was observed against *R. dentoicariosa* (Figure 8).

Typically, nanoparticles functionalized with biomolecules can be used in a variety of applications including imaging and toxicology studies, etc. Particularly, the ligands with amino and carboxylic groups are more attractive due to their excellent ability of binding to various biomaterials such as bacterial cell walls, DNAs, antibodies, etc.[64] The ligands containing surface-terminated charges such as COO^- and NH^+ effectively interact with biomolecules through various interactions such as electrostatic interaction, ionic/hydrogen bonding, and so on.[65] Although, neutral functional groups usually prevent unwanted nanomaterial−biological interactions, however, the charged ligands are more effective in interacting with biomolecules.[66] With regard to antimicrobial activities, in most of the cases, negatively charged nanoparticles have demonstrated lower uptake by bacteria.[67] Since the carboxyl, phosphate, and amino groups on the cellular membrane of the bacteria typically renders negative charge on the surfaces. This induces repulsion between the like charges and inhibits the cell-particle interaction, which reduces the toxicity of the material.[61] However, in many cases, there has been several evidences of enhanced uptake of negatively charged particles despite the unfavorable interaction between the particles and the negatively charged cell membrane.[21] For instance, investigation on the uptake of iron oxide NPs functionalized with differently charged ligands, it was revealed that the negatively charged NPs demonstrated enhanced uptake and toxicity.[68] This increased activity is attributed to the high level of internalization of NPs due to strong interactions through nonspecific binding and clustering of the particles on rarely occurred cationic sites (comparatively far less than the negatively charged anion sites) on the plasma membrane. Therefore, in this case, compared to pristine ZrO_2, which has displayed a near neutral charge (−1.78), GA-ZrO_2 has exhibited a strong negative charge (−11.9) on the surface of NPs. Particularly, at higher pH, the negative charge (−33.9) has enhanced significantly as revealed by the zeta potential study. This implies that negatively charged GA-ZrO_2 may have effectively interacted with rarely occurred positive clusters present on the surface of the bacterial cell wall, whereas the near neutral ZrO_2 could not interact efficiently. Therefore, the relatively higher antibacterial activity of GA-ZrO_2 can be attributed to the surface charge difference between functionalized and non-functionalized ZrO_2. Furthermore, the exopolysaccharide (EPS) produced by bacteria also influence the interaction between bacteria and other surfaces.[69] Since these exopolysaccharides are generally neutral, they can minimize the role of surface charges during interaction. However, being sticky in nature, they can promote binding to various surfaces. Oral pathogens tested in this study, like *S. mutans* and *Rothia mucilaginosa* are known to produce exopolysaccharides and are involved in dental carries through biofilm formation and acid production.[70] We have demonstrated earlier that *R. mucilaginosa*, which produces more EPS than *R. dentocariosa*, shows higher tolerance to ZnO NPs.[70] From the results presented in this study, it appears that the negative charge due to the functionalization with glutamic acid does not influence the binding of nanoparticles with the tested oral pathogens due to the production of EPS. Furthermore, as confirmed in the study, functionalization has improved the dispersibility increasing the nanoparticle's availability and antimicrobial activity. Furthermore, glutamic acid tested in this study is known to be involved in the acid tolerance of oral pathogen *S. mutans*.[71]

Furthermore, the pH of nanomaterial dispersion also has significant effects on the surface charges and dissolution properties of nanoparticles. Therefore, when varying the pH and improving the dispersion quality of nanoparticles, the interactions between nanoparticles and cellular constituents can be enhanced, which increase the chances of nanoparticles entering the cells.[62] For instance, in our previous study, we have demonstrated that the stabilization of nanoparticles with the phytomolecules of a plant extract enhanced the dissolution of nanoparticles in the media.[26] This has significantly enhanced

https://dx.doi.org/10.1021/acsomega.9b03840
ACS Omega 2020, 5, 1987−1996

the interactions between nanoparticles and bacterial constituents, resulting in increased antibacterial activity of plant extract-capped silver NPs. In this study, by slightly varying the pH of the medium (up to pH 8, as the antimicrobial experiments were also conducted at similar pH) in which the functionalized ZrO_2 was suspended, the surface charges of the nanoparticles in the dispersion varied significantly (increased up to −33.9), which ultimately enhanced the dispersibility of the nanoparticles in the medium. Due to this, the functionalized ZrO_2 (GA-ZrO_2) has demonstrated increased antimicrobial activity when compare to its non-functionalized counterpart.

3. MATERIALS AND METHODS

3.1. Materials. Zirconium (IV) isopropoxide isopropanol complex (99.9%), L-glutamic acid (99.0%), benzyl alcohol (99.0%), and other solvents were obtained from Sigma-Aldrich.

3.2. Synthesis of ZrO_2. The cubic ZrO_2 NPs were prepared using our previously reported method.[49,50] Briefly, 1.25 g of Zirconium (IV) isopropoxide isopropanol was added into 30 mL benzyl alcohol in a Teflon cup. The resulting mixture was vigorously stirred to completely dissolve the whole zirconium complex. The Teflon cup was fixed into a 50 mL autoclave (stainless steel) and heated to 210 °C. The reaction was stopped after 3 days (72 h), and the vessel was cooled down to obtain a turbid suspension (white). The resulting product was separated as a white crystalline powder by centrifugation. Subsequently, the product was washed with tetrahydrofuran (THF) and dried in an oven at 70 °C to obtain ZrO2 NPs.

3.3. Functionalization of ZrO_2. The as-prepared ZrO_2 NPs were functionalized using glutamic acid as the ligand in the following fashion. Initially, 15 mg of ZrO_2 NPs were taken in 10 mL benzyl alcohol; the mixture was sonicated for 20−30 min until a stable dispersion was obtained. Subsequently, the dispersion was flushed with argon gas for 30 min. Separately, 15 mg of glutamic acid was dissolved in 10 mL of benzyl alcohol, and the resultant solution was slowly poured into the ZrO_2 dispersion under gentle stirring. The mixture was allowed to stir (slow stirring) for 5 h at 50 °C. After this, the dispersion was centrifuged at 9000 rpm, and the solvent was simply removed by decanting the mixture. The sample was gently washed with ethanol (10 mL), which is removed by decanting, and the resulting biofunctionalized NPs were stored in a small amount of water or buffer solution (pH 7) for further use.

3.4. Characterization. UV measurements were performed using a Perkin-Elmer lambda 35 (Waltham, MA, USA) UV-visual spectrophotometer. The analysis was performed in quartz cuvettes using distilled water as a reference solvent. The sample for the UV measurement is obtained from a stock solution, which was prepared by diluting 1.0 mL functionalized NPs in 9 mL water via sonication for 15 min. This stock solution was further diluted by taking a 2 mL solution in 8.0 mL water. IR measurements were performed on a Perkin-Elmer 1000 (USA) Fourier transform infrared spectrometer. To remove residual or unbound glutamic acid molecules, the functionalized NPs were gently washed several times with ethanol. The sample was isolated by centrifuge at 9000 rpm for 30 min and dried in an oven for further use. Subsequently, the functionalized NPs were mixed with KBr powder to prepare the pellet for IR measurements. Background correction was made using a reference blank KBr pellet. The X-ray diffraction pattern was measured on an Altima IV [Make: Regaku, Japan] X-ray powder diffractometer using Cu Kα radiation (λ = 1.5418 Å). Meanwhile, TEM images were obtained from a JEOL JEM 1101 (USA) transmission electron microscope. The samples for TEM were prepared by placing a drop of the primary sample on a copper grid, which were dried for 6 h at 80 °C in an oven.

3.5. Bacterial Strains. Four strains of oral bacteria were used for the study namely, *R. mucilaginosa*, *R. dentocariosa*, *S. mitis*, and *S. mutans*. Some of these strains especially *S. mutans* and *R. dentocariosa* are known to cause dental caries. These strains were grown on autoclaved Brain heart infusion broth (BHI) or agar at 37 °C. Strains were stored at −80 °C in 20% glycerol for long-time storage.

3.6. Change in Antimicrobial Activity Due to Functionalization. The antimicrobial activity of functionalized and non-functionalized ZrO_2 NPs against the oral bacteria (*R. mucilaginosa*, *R. dentocariosa*, *S. mitis*, and *S. mutans*) were determined as detailed below. Cultures of the test organism were grown to the late logarithmic phase in BHI broth. Aliquots of 500 μL from the cultures of *R. mucilaginosa*, *R. dentocariosa*, *S. mitis* and *S. mutans* were inoculated in 5 mL autoclaved BHI broth. Functionalized and non-functionalized ZrO_2 NPs were added to the broths to final concentrations of 0, 200, 400, and 600 μg/mL. Tubes were incubated overnight in a rotary shaker at 37 °C. Samples grown to the log phase in the presence of the test compounds were diluted in autoclaved phosphate-buffered saline (pH, 7.0) following incubation. Also, aliquots of 100 μL from the appropriate dilutions were spread on agar plates, and plates were incubated at 37 °C for 2−3 days. After incubation, colony-forming units were determined and plotted using the Sigma plot (Systat Software Inc., London, UK). Values presented are the mean and standard deviation of three values.

3.7. Assessment of Biofilm Formation. Quantitative assessment of biofilm formation and its inhibition in the presence of functionalized and non-functionalized ZrO_2 NPs was performed on 48-well polystyrene plates (Nunc, Denmark) using the protocol of Burton et al.[72] An aliquot of 500 μL from overnight-grown cultures of the test strain was added to sterile BHI broth containing 100, 200, 300,400, and 500 μg/mL of functionalized and non-functionalized ZrO_2 NPs (v/v). Cultures without NPs were taken as the control. These plates were incubated at 37 °C for 48 h for biofilm formation. The medium containing suspended cells was gently removed, and wells were washed three times with 500 μL of PBS (pH 7.4). Plates were air-dried for 15 min and stained with 500 μL of 0.4% crystal violet (CV) dye for 15 min at room temperature. Wells were washed gently three times with 500 μL of PBS buffer to remove any unbound dye. The CV retained by the biofilm was dissolved in 500 μL of 33% acetic acid. The absorption at 620 nm was recorded using a microtiter plate reader (Multiskan Ascent, Labsystems, Helsinki, Finland).

3.8. Statistical Analysis. The results presented are the mean ± standard error of two independent experiments done in triplicate. GraphPad Prism version 5.0 (GraphPad Software, Inc. USA) was used to attain statistical significance through the Mann−Whitney unpaired *t* test.

4. CONCLUSIONS

In this study, we have successfully altered the surface properties of solvothermally prepared ZrO_2 NPs using glutamic acid (GA) as the stabilizing agent. The biofunction-

https://dx.doi.org/10.1021/acsomega.9b03840
ACS Omega 2020, 5, 1987−1996

alized GA-ZrO_2 has demonstrated an increased dispersibility and enhanced antimicrobial activities. GA is an α-amino acid consisting of both COO^- and NH^+ ions, which facilitated the binding of the ligand with the surfaces of ZrO_2 NPs. The biomolecule interacted with the ZrO_2 through its NH^+ moiety, leaving its COO^- group suspended, which has rendered a stable negative charge on the surface of NPs. Furthermore, the negative charge increased substantially at a slightly higher pH (pH 8), which has led to an enhanced dispersibility of GA-ZrO_2 in aqueous media. The stable negative charge and superior dispersion quality of GA-ZrO_2 has facilitated the effective interaction of NPs with the bacterial cell wall. These interactions may have occurred through electrostatic attraction between surface-terminated negatively charged COO^- groups of GA and rarely occurred positive clusters on the bacterial cell wall.

■ ASSOCIATED CONTENT

Supporting Information

The Supporting Information is available free of charge at https://pubs.acs.org/doi/10.1021/acsomega.9b03840.

Zeta potential plots of ZrO_2, GA-ZrO_2, and ZrO_2 and GA-ZrO_2 at pH 8, XRD spectrum of pure ZrO_2 and TEM images of pure ZrO_2 at different resolutions (PDF)

■ AUTHOR INFORMATION

Corresponding Authors

Mujeeb Khan − *Department of Chemistry, College of Science, King Saud University, Riyadh 11451, Kingdom of Saudi Arabia*; orcid.org/0000-0002-4088-6913; Email: kmujeeb@ksu.edu.sa

Muhammad Nawaz Tahir − *Chemistry Department, King Fahd University of Petroleum & Minerals, Dhahran 31261, Kingdom of Saudi Arabia*; Email: muhammad.tahir@kfupm.edu.sa

Authors

Mohammed Rafi Shaik − *Department of Chemistry, College of Science, King Saud University, Riyadh 11451, Kingdom of Saudi Arabia*

Shams Tabrez Khan − *Department of Agricultural Microbiology, Faculty of Agriculture, Aligarh Muslim University, Aligarh 202002, India*

Syed Farooq Adil − *Department of Chemistry, College of Science, King Saud University, Riyadh 11451, Kingdom of Saudi Arabia*

Mufsir Kuniyil − *Department of Chemistry, Koneru Lakshmaiah Education Foundation, Guntur 522502, India*; orcid.org/0000-0001-8038-1381

Majad Khan − *Chemistry Department, King Fahd University of Petroleum & Minerals, Dhahran 31261, Kingdom of Saudi Arabia*

Abdulrahman A. Al-Warthan − *Department of Chemistry, College of Science, King Saud University, Riyadh 11451, Kingdom of Saudi Arabia*

Mohammed Rafiq H. Siddiqui − *Department of Chemistry, College of Science, King Saud University, Riyadh 11451, Kingdom of Saudi Arabia*

Complete contact information is available at: https://pubs.acs.org/10.1021/acsomega.9b03840

Author Contributions

Mu.K., M.N.T., and S.F.A. designed the project. Mu.K., S.F.A., M.N.T. and M.R.S. helped draft the manuscript. M.R.S. and M.K. carried out the experimental part and some parts of characterization. S.T.K. carried out the antimicrobial activity. A.Al-W. and M.R.H.S. provided scientific guidance for successful completion of the project and also helped draft the manuscript. All authors read and approved the final manuscript.

Notes

The authors declare no competing financial interest.

■ ACKNOWLEDGMENTS

The authors extend their appreciation to the Deanship of Scientific Research at King Saud University for funding this work through the research group project no. RG-1436-032.

■ REFERENCES

(1) Leibovici, L.; Paul, M.; Garner, P.; Sinclair, D. J.; Afshari, A.; Pace, N. L.; Cullum, N.; Williams, H. C.; Smyth, A.; Skoetz, N.; Del Mar, C.; Schilder, A. G. M.; Yahav, D.; Tovey, D. Addressing resistance to antibiotics in systematic reviews of antibiotic interventions. *J. Antimicrob. Chemother.* **2016**, *71*, 2367−2369.

(2) Mingeot-Leclercq, M.-P.; Décout, J.-L. Bacterial lipid membranes as promising targets to fight antimicrobial resistance, molecular foundations and illustration through the renewal of aminoglycoside antibiotics and emergence of amphiphilic aminoglycosides. *MedChemComm* **2016**, *7*, 586−611.

(3) Cohen, N. R.; Lobritz, M. A.; Collins, J. J. Microbial persistence and the road to drug resistance. *Cell Host Microbe* **2013**, *13*, 632−642.

(4) Ding, X.; Duan, S.; Ding, X.; Liu, R.; Xu, F.-J. Versatile Antibacterial Materials: An Emerging Arsenal for Combatting Bacterial Pathogens. *Adv. Funct. Mater.* **2018**, *28*, 1802140.

(5) Laxminarayan, R.; Duse, A.; Wattal, C.; Zaidi, A. K. M.; Wertheim, H. F. L.; Sumpradit, N.; Vlieghe, E.; Hara, G. L.; Gould, I. M.; Goossens, H.; Greko, C.; So, A. D.; Bigdeli, M.; Tomson, G.; Woodhouse, W.; Ombaka, E.; Peralta, A. Q.; Qamar, F. N.; Mir, F.; Kariuki, S.; Bhutta, Z. A.; Coates, A.; Bergstrom, R.; Wright, G. D.; Brown, E. D.; Cars, O. Antibiotic resistance—the need for global solutions. *Lancet Infect. Dis.* **2013**, *13*, 1057−1098.

(6) Huh, A. J.; Kwon, Y. J. "Nanoantibiotics": a new paradigm for treating infectious diseases using nanomaterials in the antibiotics resistant era. *J. Controlled Release* **2011**, *156*, 128−145.

(7) Xia, Y. Nanomaterials at work in biomedical research. *Nat. Mater.* **2008**, *7*, 758.

(8) Wang, Y.; Jin, Y.; Chen, W.; Wang, J.; Chen, H.; Sun, L.; Li, X.; Ji, J.; Yu, Q.; Shen, L.; Wang, B. Construction of nanomaterials with targeting phototherapy properties to inhibit resistant bacteria and biofilm infections. *Chem. Eng. J.* **2019**, *358*, 74−90.

(9) Hajipour, M. J.; Fromm, K. M.; Ashkarran, A. A.; de Aberasturi, D. J.; de Larramendi, I. R.; Rojo, T.; Serpooshan, V.; Parak, W. J.; Mahmoudi, M. Antibacterial properties of nanoparticles. *Trends Biotechnol.* **2012**, *30*, 499−511.

(10) Stoimenov, P. K.; Klinger, R. L.; Marchin, G. L.; Klabunde, K. J. Metal oxide nanoparticles as bactericidal agents. *Langmuir* **2002**, *18*, 6679−6686.

(11) Li, Y.; Zhang, W.; Niu, J.; Chen, Y. Mechanism of photogenerated reactive oxygen species and correlation with the antibacterial properties of engineered metal-oxide nanoparticles. *ACS Nano* **2012**, *6*, 5164−5173.

(12) Siegel, J.; Kolářová, K.; Vosmanská, V.; Rimpelová, S.; Leitner, J.; Švorčík, V. Antibacterial properties of green-synthesized noble metal nanoparticles. *Mater. Lett.* **2013**, *113*, 59−62.

(13) Khan, S. T.; Musarrat, J.; Al-Khedhairy, A. A. Countering drug resistance, infectious diseases, and sepsis using metal and metal oxides nanoparticles: current status. *Colloids Surf., B Biointerfaces* **2016**, *146*, 70−83.

(14) Durán, N.; Durán, M.; de Jesus, M. B.; Seabra, A. B.; Fávaro, W. J.; Nakazato, G. Silver nanoparticles: A new view on mechanistic aspects on antimicrobial activity. *Nanomed.: Nanotechnol. Biol. Med.* **2016**, *12*, 789−799.
(15) Ravindran, A.; Chandran, P.; Khan, S. S. Biofunctionalized silver nanoparticles: advances and prospects. *Colloids Surf., B* **2013**, *105*, 342−352.
(16) Wei, T.; Yu, Q.; Chen, H. Responsive and Synergistic Antibacterial Coatings: Fighting against Bacteria in a Smart and Effective Way. *Adv. Healthcare Mater.* **2019**, *8*, 1801381.
(17) Dickson, J. S.; Koohmaraie, M. Cell surface charge characteristics and their relationship to bacterial attachment to meat surfaces. *Appl. Environ. Microbiol.* **1989**, *55*, 832−836.
(18) Vu, B.; Chen, M.; Crawford, R.; Ivanova, E. Bacterial extracellular polysaccharides involved in biofilm formation. *Molecules* **2009**, *14*, 2535−2554.
(19) Alarcon, E. I.; Udekwu, K.; Skog, M.; Pacioni, N. L.; Stamplecoskie, K. G.; González-Béjar, M.; Polisetti, N.; Wickham, A.; Richter-Dahlfors, A.; Griffith, M.; Scaiano, J. C. The biocompatibility and antibacterial properties of collagen-stabilized, photochemically prepared silver nanoparticles. *Biomaterials* **2012**, *33*, 4947−4956.
(20) Kawai, K.; Narushima, T.; Kaneko, K.; Kawakami, H.; Matsumoto, M.; Hyono, A.; Nishihara, H.; Yonezawa, T. Synthesis and antibacterial properties of water-dispersible silver nanoparticles stabilized by metal−carbon σ-bonds. *Appl. Surf. Sci.* **2012**, *262*, 76−80.
(21) Verma, A.; Stellacci, F. Effect of surface properties on nanoparticle−cell interactions. *Small* **2010**, *6*, 12−21.
(22) Shaik, M.; Albalawi, G.; Khan, S.; Khan, M.; Adil, S.; Kuniyil, M.; Al-Warthan, A.; Siddiqui, M.; Alkhathlan, H.; Khan, M. "Miswak" based green synthesis of silver nanoparticles: Evaluation and comparison of their microbicidal activities with the chemical synthesis. *Molecules* **2016**, *21*, 1478.
(23) Mei, Z.; Dhanale, A.; Gangaharan, A.; Sardar, D. K.; Tang, L. Water dispersion of magnetic nanoparticles with selective Biofunctionality for enhanced plasmonic biosensing. *Talanta* **2016**, *151*, 23−29.
(24) Mout, R.; Moyano, D. F.; Rana, S.; Rotello, V. M. Surface functionalization of nanoparticles for nanomedicine. *Chem. Soc. Rev.* **2012**, *41*, 2539−2544.
(25) Weissman, M. R.; Winger, K. T.; Ghiassian, S.; Gobbo, P.; Workentin, M. S. Insights on the application of the retro Michael-type addition on maleimide-functionalized gold nanoparticles in biology and nanomedicine. *Bioconjugate Chem.* **2016**, *27*, 586−593.
(26) Alkhathlan, H.; Khan, M.; Khan, S. T.; Khan, M.; Adil, S. F.; Musarrat, J.; Al-Warthan, A.; Siddiqui, M. R. H.; Al-Khedhairy, A. A. Antibacterial properties of silver nanoparticles synthesized using Pulicaria glutinosa plant extract as a green bioreductant. *Int. J. Nanomedicine* **2014**, *9*, 3551−3565.
(27) Thanh, N. T. K.; Green, L. A. W. Functionalisation of nanoparticles for biomedical applications. *Nano Today* **2010**, *5*, 213−230.
(28) Shen, C.; Lan, X.; Lu, X.; Meyer, T. A.; Ni, W.; Ke, Y.; Wang, Q. Site-specific surface functionalization of gold nanorods using DNA origami clamps. *J. Am. Chem. Soc.* **2016**, *138*, 1764−1767.
(29) Veerapandian, M.; Yun, K. Functionalization of biomolecules on nanoparticles: specialized for antibacterial applications. *Appl. Microbiol. Biotechnol.* **2011**, *90*, 1655−1667.
(30) Bose, R. J. C.; Lee, S.-H.; Park, H. Biofunctionalized nanoparticles: an emerging drug delivery platform for various disease treatments. *Drug Discovery Today* **2016**, *21*, 1303−1312.
(31) Malassis, L.; Dreyfus, R.; Murphy, R. J.; Hough, L. A.; Donnio, B.; Murray, C. B. One-step green synthesis of gold and silver nanoparticles with ascorbic acid and their versatile surface post-functionalization. *RSC Adv.* **2016**, *6*, 33092−33100.
(32) Anami, Y.; Yamazaki, C. M.; Xiong, W.; Gui, X.; Zhang, N.; An, Z.; Tsuchikama, K. Glutamic acid−valine−citrulline linkers ensure stability and efficacy of antibody−drug conjugates in mice. *Nat. Commun.* **2018**, *9*, 2512.
(33) Foley, P.; Kermanshahi pour, A.; Beach, E. S.; Zimmerman, J. B. Derivation and synthesis of renewable surfactants. *Chem. Soc. Rev.* **2012**, *41*, 1499−1518.
(34) Stephen Inbaraj, B.; Kao, T. H.; Tsai, T. Y.; Chiu, C. P.; Kumar, R.; Chen, B. H. The synthesis and characterization of poly(γ-glutamic acid)-coated magnetite nanoparticles and their effects on antibacterial activity and cytotoxicity. *Nanotechnology* **2011**, *22*, No. 075101.
(35) Chen, Y.; Fu, G.; Li, Y.; Gu, Q.; Xu, L.; Sun, D.; Tang, Y. l-Glutamic acid derived PtPd@Pt core/satellite nanoassemblies as an effectively cathodic electrocatalyst. *J. Mater. Chem. A* **2017**, *5*, 3774−3779.
(36) Zhu, Y.; Kekalo, K.; NDong, C.; Huang, Y.-Y.; Shubitidze, F.; Griswold, K. E.; Baker, I.; Zhang, J. X. J. Magnetic-Nanoparticle-Based Immunoassays-on-Chip: Materials Synthesis, Surface Functionalization, and Cancer Cell Screening. *Adv. Funct. Mater.* **2016**, *26*, 3953−3972.
(37) Gupta, A.; Moyano, D. F.; Parnsubsakul, A.; Papadopoulos, A.; Wang, L.-S.; Landis, R. F.; Das, R.; Rotello, V. M. Ultrastable and biofunctionalizable gold nanoparticles. *ACS Appl. Mater. Interfaces* **2016**, *8*, 14096−14101.
(38) Pazos, E.; Sleep, E.; Rubert Pérez, C. M.; Lee, S. S.; Tantakitti, F.; Stupp, S. I. Nucleation and growth of ordered arrays of silver nanoparticles on peptide nanofibers: hybrid nanostructures with antimicrobial properties. *J. Am. Chem. Soc.* **2016**, *138*, 5507−5510.
(39) Azam, A.; Ahmed, A. S.; Oves, M.; Khan, M. S.; Habib, S. S.; Memic, A. Antimicrobial activity of metal oxide nanoparticles against Gram-positive and Gram-negative bacteria: a comparative study. *Int. J. Nanomed.* **2012**, *7*, 6003−6009.
(40) Raghunath, A.; Perumal, E. Metal oxide nanoparticles as antimicrobial agents: a promise for the future. *Int. J. Antimicrob. Agents* **2017**, *49*, 137−152.
(41) Gopinath, V.; Priyadarshini, S.; Al-Maleki, A. R.; Alagiri, M.; Yahya, R.; Saravanan, S.; Vadivelu, J. In vitro toxicity, apoptosis and antimicrobial effects of phyto-mediated copper oxide nanoparticles. *RSC Adv.* **2016**, *6*, 110986−110995.
(42) Liu, Y.; He, L.; Mustapha, A.; Li, H.; Hu, Z. Q.; Lin, M. Antibacterial activities of zinc oxide nanoparticles against Escherichia coli O157:H7. *J. Appl. Microbiol.* **2009**, *107*, 1193−1201.
(43) Al-Radha, A. S. D.; Dymock, D.; Younes, C.; O'Sullivan, D. Surface properties of titanium and zirconia dental implant materials and their effect on bacterial adhesion. *J. Dent.* **2012**, *40*, 146−153.
(44) Jangra, S. L.; Stalin, K.; Dilbaghi, N.; Kumar, S.; Tawale, J.; Singh, S. P.; Pasricha, R. Antimicrobial Activity of Zirconia (ZrO2) Nanoparticles and Zirconium Complexes. *J. Nanosci. Nanotechnol.* **2012**, *12*, 7105−7112.
(45) Sadeek, S. A.; El-Shwiniy, W. H.; Zordok, W. A.; El-Didamony, A. M. Spectroscopic, structure and antimicrobial activity of new Y(III) and Zr(IV) ciprofloxacin. *Spectrochim. Acta, Part A* **2011**, *78*, 854−867.
(46) Liu, Y.-T.; Lee, T.-M.; Lui, T.-S. Enhanced osteoblastic cell response on zirconia by bio-inspired surface modification. *Colloids Surf., B* **2013**, *106*, 37−45.
(47) Kumaresan, M.; Vijai Anand, K.; Govindaraju, K.; Tamilselvan, S.; Ganesh Kumar, V. Seaweed Sargassum wightii mediated preparation of zirconia (ZrO_2) nanoparticles and their antibacterial activity against gram positive and gram negative bacteria. *Microb. Pathog.* **2018**, *124*, 311−315.
(48) Liu, M.; Zhou, J.; Yang, Y.; Zheng, M.; Yang, J.; Tan, J. Surface modification of zirconia with polydopamine to enhance fibroblast response and decrease bacterial activity in vitro: A potential technique for soft tissue engineering applications. *Colloids Surf., B* **2015**, *136*, 74−83.
(49) Shaik, M.; Alam, M.; Adil, S.; Kuniyil, M.; Al-Warthan, A.; Siddiqui, M.; Tahir, M.; Labis, J.; Khan, M. Solvothermal Preparation and Electrochemical Characterization of Cubic ZrO_2 Nanoparticles/Highly Reduced Graphene (HRG) based Nanocomposites. *Materials* **2019**, *12*, 711.

https://dx.doi.org/10.1021/acsomega.9b03840
ACS Omega 2020, 5, 1987−1996

(50) Shaik, M. R.; Al-Marri, A. H.; Adil, S. F.; Mohri, N.; Barton, B.; Siddiqui, M. R. H.; Al-Warthan, A.; Labis, J. P.; Tremel, W.; Khan, M.; Tahir, M. N. Benzyl alcohol assisted synthesis and characterization of highly reduced graphene oxide (HRG)@ ZrO_2 nanocomposites. *ChemistrySelect* **2017**, *2*, 3078−3083.
(51) Wangoo, N.; Bhasin, K. K.; Mehta, S. K.; Suri, C. R. Synthesis and capping of water-dispersed gold nanoparticles by an amino acid: Bioconjugation and binding studies. *J. Colloid Interface Sci.* **2008**, *323*, 247−254.
(52) Dubey, S. K.; Sharma, A. K.; Narain, U.; Misra, K.; Pati, U. Design, synthesis and characterization of some bioactive conjugates of curcumin with glycine, glutamic acid, valine and demethylenated piperic acid and study of their antimicrobial and antiproliferative properties. *Eur. J. Med. Chem.* **2008**, *43*, 1837−1846.
(53) Kumirska, J.; Czerwicka, M.; Kaczyński, Z.; Bychowska, A.; Brzozowski, K.; Thöming, J.; Stepnowski, P. Application of Spectroscopic Methods for Structural Analysis of Chitin and Chitosan. *Marine Drugs* **2010**, *8*, 1567−1636.
(54) Rajh, T.; Chen, L. X.; Lukas, K.; Liu, T.; Thurnauer, M. C.; Tiede, D. M. Surface restructuring of nanoparticles: an efficient route for ligand−metal oxide crosstalk. *J. Phys. Chem. B* **2002**, *106*, 10543−10552.
(55) Tahir, M. N.; Theato, P.; Oberle, P.; Melnyk, G.; Faiss, S.; Kolb, U.; Janshoff, A.; Stepputat, M.; Tremel, W. Facile synthesis and characterization of functionalized, monocrystalline rutile TiO_2 nanorods. *Langmuir* **2006**, *22*, 5209−5212.
(56) Heacock, R. A.; Marion, L. The infrared spectra of secondary amines and their salts. *Can. J. Chem.* **1956**, *34*, 1782−1795.
(57) Purohit, R.; Venugopalan, P. Polymorphism: an overview. *Resonance* **2009**, *14*, 882.
(58) Dharmayat, S.; De Anda, J. C.; Hammond, R. B.; Lai, X.; Roberts, K. J.; Wang, X. Z. Polymorphic transformation of l-glutamic acid monitored using combined on-line video microscopy and X-ray diffraction. *J. Cryst. Growth* **2006**, *294*, 35−40.
(59) Moshe, H.; Levi, G.; Mastai, Y. Polymorphism stabilization by crystal adsorption on a self-assembled monolayer. *CrystEngComm* **2013**, *15*, 9203−9209.
(60) Chandra, A.; Singh, M. Biosynthesis of amino acid functionalized silver nanoparticles for potential catalytic and oxygen sensing applications. *Inorg. Chem. Front.* **2018**, 233.
(61) El Badawy, A. M.; Silva, R. G.; Morris, B.; Scheckel, K. G.; Suidan, M. T.; Tolaymat, T. M. Surface Charge-Dependent Toxicity of Silver Nanoparticles. *Environ. Sci. Technol.* **2011**, *45*, 283−287.
(62) Berg, J. M.; Romoser, A.; Banerjee, N.; Zebda, R.; Sayes, C. M. The relationship between pH and zeta potential of ∼ 30 nm metal oxide nanoparticle suspensions relevant to in vitro toxicological evaluations. *Nanotoxicology* **2009**, *3*, 276−283.
(63) Fujii, S.; Kido, M.; Sato, M.; Higaki, Y.; Hirai, T.; Ohta, N.; Kojio, K.; Takahara, A. pH-Responsive and selective protein adsorption on an amino acid-based zwitterionic polymer surface. *Polym. Chem.* **2015**, *6*, 7053−7059.
(64) Han, G.-M.; Jiang, H.-X.; Huo, Y.-F.; Kong, D.-M. Simple synthesis of amino acid-functionalized hydrophilic upconversion nanoparticles capped with both carboxyl and amino groups for bimodal imaging. *J. Mater. Chem. B* **2016**, *4*, 3351−3357.
(65) Bohara, R. A.; Thorat, N. D.; Pawar, S. H. Role of functionalization: strategies to explore potential nano-bio applications of magnetic nanoparticles. *RSC Adv.* **2016**, *6*, 43989−44012.
(66) Feng, Z. V.; Gunsolus, I. L.; Qiu, T. A.; Hurley, K. R.; Nyberg, L. H.; Frew, H.; Johnson, K. P.; Vartanian, A. M.; Jacob, L. M.; Lohse, S. E.; Torelli, M. D.; Hamers, R. J.; Murphy, C. J.; Haynes, C. L. Impacts of gold nanoparticle charge and ligand type on surface binding and toxicity to Gram-negative and Gram-positive bacteria. *Chem. Sci.* **2015**, *6*, 5186−5196.
(67) Pillai, P. P.; Kowalczyk, B.; Kandere-Grzybowska, K.; Borkowska, M.; Grzybowski, B. A. Engineering Gram Selectivity of Mixed-Charge Gold Nanoparticles by Tuning the Balance of Surface Charges. *Angew. Chem., Int. Ed.* **2016**, *55*, 8610−8614.
(68) Villanueva, A.; Cañete, M.; Roca, A. G.; Calero, M.; Veintemillas-Verdaguer, S.; Serna, C. J.; del Puerto Morales, M.; Miranda, R. The influence of surface functionalization on the enhanced internalization of magnetic nanoparticles in cancer cells. *Nanotechnology* **2009**, *20*, 115103.
(69) Khan, S. T.; Al-Khedhairy, A. A.; Musarrat, J. ZnO and TiO_2 nanoparticles as novel antimicrobial agents for oral hygiene: a review. *J. Nanopart. Res.* **2015**, *17*, 276.
(70) Khan, S. T.; Ahamed, M.; Musarrat, J.; Al-Khedhairy, A. A. Anti-biofilm and antibacterial activities of zinc oxide nanoparticles against the oral opportunistic pathogens Rothia dentocariosa and Rothia mucilaginosa. *Eur. J. Oral Sci.* **2014**, *122*, 397−403.
(71) Krastel, K.; Senadheera, D. B.; Mair, R.; Downey, J. S.; Goodman, S. D.; Cvitkovitch, D. G. Characterization of a glutamate transporter operon, *glnQHMP*, in *Streptococcus mutans* and its role in acid tolerance. *J. Bacteriol.* **2010**, *192*, 984−993.
(72) Burton, E.; Yakandawala, N.; LoVetri, K.; Madhyastha, M. A microplate spectrofluorometric assay for bacterial biofilms. *J. Ind. Microbiol. Biotechnol.* **2007**, *34*, 1−4.

https://dx.doi.org/10.1021/acsomega.9b03840
ACS Omega 2020, 5, 1987−1996